Dalton Transactions

Accepted Manuscript

ROYAL SOCIETY OF CHEMISTRY

www.rsc.org/dalton

Cite this: DOI: 10.1039/c0xx00000x

www.rsc.org/xxxxxx

ARTICLE TYPE

Microwave-assisted synthesis of arene ruthenium(II) complexes [(η^6-RC_6H_5)Ru(*m*-MOPIP)Cl]Cl (R= -H and -CH_3) as groove binder to *c-myc* G4 DNA

Qiong Wu,[#a] Tianfeng Chen,[#b] Zhao Zhang,[a] Siyan Liao,[c] Xiaohui Wu,[a] Jian Wu,[a] Wenjie Mei,[*ab] Yanhua Chen,[a] Weili Wu,[a] Lingli Zeng,[a] and Wenjie Zheng[*b]

Received (in XXX, XXX) Xth XXXXXXXXX 20XX, Accepted Xth XXXXXXXXX 20XX
DOI: 10.1039/b000000x

Two arene Ru(II) complexes coordinated by 2-(3-methoxyphenyl)imidazole[4,5*f*][1,10] phenanthroline, [(η^6-RC_6H_5)Ru(*m*-MOPIP)Cl]Cl (R = H, **1**; R =CH_3, **2**) have been prepared under the microwave irradiation, and the crystal structure of **2** exhibits a typical "piano stool" conformation, with the bond angles for N1–Ru1–Cl1 (86.02 (14)°) and N2–Ru1–Cl1 (84.51 (14)°). The Ru–C distance for Ru atom bond to the benzene ring is about 0.2175 (6.5) nm, and the average Ru–N distance for Ru atom to the two chelating N atoms is about 0.2092 (4) nm. The evaluation of in vitro anticancer activities revealed that these synthetic Ru(II) complexes selectively inhibited the growth of HepG2 hepatocellular carcinoma cells, with low cytotoxicity toward LO2 human normal liver cells. The results demonstrated that the omplexes exhibited great selectivity between human cancer and normal cells by comparing with the ligand *m*-MOPIP. Furthermore, complexes **1** and **2** could bind to *c-myc* G4 DNA in groove binding mode in promising affinity, and the insertion of methyl groups in arene ligand contribute to strengthen the binding affinity. This was aslo confirmed by molecular docking calculation and ^{1}H NMR analysis which show that both **1** and **2** can bind in the loop constructed by base pairs of A6~G9 and G21~A25 in *c-myc* G4 DNA to block the replication of *c-myc* oligomer. Taken together, these results suggest that arene Ru(II) complexes display application potential as small molecule inhibitors of *c-myc* G4 DNA.

Introduction

For years, G-quadruplex DNA, especially the oncogene *c-myc* which is closely associated with cell-cycle regulation, proliferation and growth of tumor cells, has been considered as a potential target for antitumor drugs.[1] Those small molecules, such as porphyrin, quindoline and quarfloxin, have an inhibitory effect on various tumor cells by stabilizing the G-quadruplex DNA.[2] Furthermore, there is a clear evidence that Ru complexes can bind strongly to G-quadruplex DNA and induce apoptosis of tumor cells. For example, ruthenium (Ru)-porphyrin complex [$Ru(phen)_2$MPyTPP] (phen = phenanthroline, MPyTPP =*mono*-(*3'*-Pyridine)-10,15,20-triphenylporphyrin) exhibits high affinity to G-quadruplex DNA and inhibits growth of tumor cells.[3] Zimbron has reported that Ru complex assembled by presenter protein binds more strongly to telomere G-quadruplex DNA than to double-stranded DNA.[4] More recently, a number of ruthenium(II) polypyridyl complexes, such as containing dppz, ptpn and bqdppz ligand, have also been reported to selectively bind to telomeric G-quadruplex DNA by π-π stacking.[5] Besides, there are also some researches focus on the interaction of arene Ru(II) complexes with telomeric G-quadruplex DNA but with few reports about binding mode.[6] However, there is little information available on the interaction of arene Ru(II) complexes with *c-myc* G-quadruplex DNA, which is a key factor regulated the development of tumor, and to understand this is helpful in the design of novel anticancer drugs with high activity and selectivity.

On the other hand, arene Ru(II) complexes have long been considered as one of the most promising candidates for anticancer drugs since NAMI-A and KP1019 entered into clinical trials. A number of arene Ru(II) complexes with high antitumor activity and low toxixcity to human normal cells has kindled great interest of scientists.[7] It's reported that arene Ru(II) complexes may inhibit the growth of tumor cells by inducing cell-cycle arrest, DNA damage and apoptosis of tumor cells.[8] Dyson reported that RAPTA-C (η^6-*p*-$MeC_6H_4Pr^i$)Ru(PTA)Cl_2, PTA=1,3,5-triaza-7-hosphaadamantane) inhibits the growth of tumor cells by inducing cell-cycle arrest in G2/M phase.[9] Furthermore, arene Ru(II) complexes coordinated by curcumin, with their high affinity to DNA molecules, also inhibit the growth of tumor cells *via* proteasome inhibition and apoptosis induction.[10] In recently, arene Ru(II) complex modified by nanoscaled carborane have also been reported to induce apoptosis of human lung cancer cells

significantly as indicated by a high cleaved Caspase-8,9 ratio.[11] Our previous studies have also found that arene Ru(II) complexes coordinated with phenanthroimidazole derivatives exhibit a considerable antitumor activity by inducing S-phase arrest mediated by DNA damage in tumor cells.[12]

In this study, two arene Ru(II) complexes coordinated by 2-(3-methoxyphenyl)imidazole[4,5*f*][1,10]phenanthroline have been synthesized under microwave irradiation. The antitumor activity of **1** and **2** against human liver cancer HepG2 cells and the toxicity to normal human liver LO2 cells were evaluated by MTT, the results showed that both complexes exhibited acceptable antitumor activity and low toxicity. The interactions of **1** and **2** with *c-myc* G4 DNA were further investigated to show that **1** and **2** can stabilize the conformation of G-quadruplex DNA *via* groove binding mode, indicating their potential utility in chemotherapy by targeting to *c-myc* G4 DNA.

Results and Discussion

Microwave-assisted Synthesis of arene Ru(II) complexes

The synthesis of arene Ru(II) complexes of the general formulations [(η^6-RC_6H_5)Ru(*m*-MOPIP)Cl]Cl (where R=-H, **1**; -CH_3, **2**) has been achieved by the reaction of chloro-bridged dimeric compound [(η^6- RC_6H_5)$RuCl_2$]$_2$ (R = -H, for **1**; -CH_3, for **2**) with 2-(3-methoxyphenyl)imidazole[4,5*f*][1,10]phenanthroline (***m*-MOPIP**), under microwave irradiation in the SiC vessel. SiC is a ceramic material adsorbing microwave irradiation and transforming it to heat instantly.[13] The SiC vessel and the reaction profile of the arene ruthenium(II) complexes synthesis are shown in **Scheme S1**, and the yields of **1** and **2** are listed in **Table S1**.

X-ray Structure of the complexes.

Crystals of complex **1** and **2** suitable for an X-ray crystal-structure determination were obtained from DMF-MeOH (1:9) solution by slow evaporation of the solvent at room temperature. The molecular structure of the lattice for **1** and **2** are illustrated in **Figure 1** and the selected crystallographic data, selected bond distances, and bond angles are listed in Table S1 and Table S2.

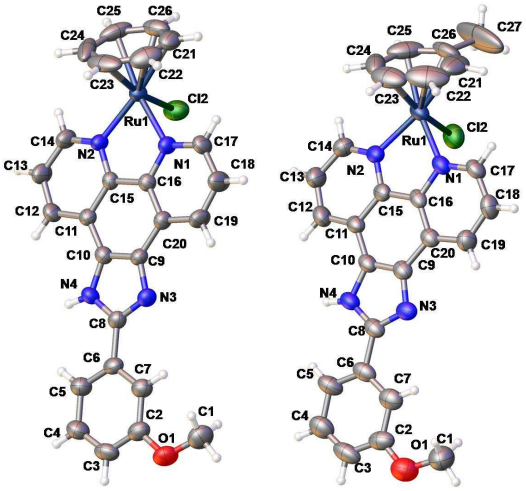

Fig.1 The molecular structure of the lattice and the atom numbers of **1** and **2**

As shown in **Fig. 1**, **1** adopts the typical "piano stool" structure as demonstrated by the nearly 90° bond angles for N1–Ru1–Cl1 (86.02 (14)°) and N2–Ru1–Cl1 (84.51 (14)°).[12] The Ru atom bond to the benzene ring has an average Ru–C distance of 0.2175 (6.5) nm, whereas the average distance of Ru to the two chelating nitrogen atoms is 0.2092 (4) nm. The same thing was occured for **2**, while subtle differences in bond length and bond angle attribute to the presence of the methyl group.

Table 1. Inhibitory effect of arene Ru(II) complexes on human liver cancer and normal cells.

Complex	IC_{50} (μM)		Toxicity index*
	HepG2	LO2	
1	48.8	212.4	4.4
2	43.7	129.1	2.9
m-MOPIP	42.2	34.9	0.83

* Toxicity index = IC_{50} (LO2)/ IC_{50} (HepG2).

Arene Ru(II) complexes exhibit selectivity between cancer and normal cells

The antitumor activity of both arene Ru(II) complexes were screened against human liver cancer HepG2 cells and normal LO2 cells by MTT assay. The inhibitory effects of the synthetic arene Ru(II) complexes and the ligand *m*-MOPIP on various cell lines after 72 h treatment were demonstrated. As shown in **Table 1**, both arene Ru(II) complexes **1** and **2** displayed acceptable antiproliferative activity against human liver HepG2 cells with IC_{50} values at 48.8 and 43.7 μM, respectiviely, which are comparable with those of the ligand *m*-MOPIP under the same conditions. Importantly, we found that, the complexes exhibited lower toxicity toward normal human liver LO2 cells with IC_{50} at 212.4 and 129.1 μM, respectively. Thus, the toxicity index of **1** and **2** is about 4.4 and 2.9, respectively. These values are far higher than that of *m*-MOPIP (0.83), indicating the lower toxicity on LO2 cells. Martinez *et al* reported a series of arene-Ru(II)-chloroquine complexes, which exhibited great inhibition to human lymphoid tumor cells by induction of apoptosis and low toxicity to normal human foreskin fibroblast cells.[8g] Comparison with arene–Ru(II)–chloroquine complexes, we also found that the synthetic arene Ru complexes are more sensitively to tumor cells and equally or less toxic to normal human liver cells than ligand *m*-MOPIP, and demonstrate application potential in treatment of human cancers.

Bingding behaviours of arene Ru(II) complexes with *c-myc* G4 DNA.

Oncogene *c-myc*, associated with advanced malignancy and poor prognosis, is among the most abundantly overexpressed genes in human tumor cells.[14] The guanine rich promoter of *c-myc* can form a G-quadruplex conformation *via* Hoogsten hydrogen bond,[15] and the inhibitors which bind to *c-myc* G4-DNA can repress the expression of c-Myc.[16] The interactions of both arene Ru(II) complexes with *c-myc* G4 DNA have been evaluated by electronic spectra, emission spectra, ITC and FRET, as well as using CD spectra, molecular docking, ^{1}H NMR Analysis and PCR-stop methods.

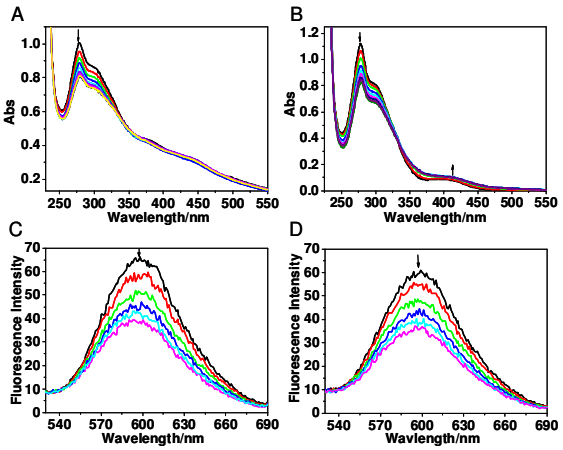

Fig.2 The study of interaction between arene Ru(II) **1** and **2** with *c-myc* G4 DNA by Spectroscopic methods. The electronic spectra of arene Ru(II) complex **1** (A) and **2** (B) in the absence and presence of *c-myc* G4 DNA, [Ru] = 20 μM. Emission spectra of EB and *c-myc* G4 DNA in the incubation buffer in the absence and presence of **1** (C) and **2** (D), [EB] = 16 μM, [DNA] = 2 μM.

The electronic spectra are one of the most common methods to study the interaction of transition metal complexes with biological molecules. In general, transition metal complexes, especially ruthenium complexes, have broad spectroscopic properties which undergo hypochromism and red shift in the presence of biological molecules. The severity of such changes depends on the binding ability of the compounds.[17] The electronic spectra of **1** and **2** in the absence and in presence of *c-myc* G4 DNA are illustrated in Figure 2A and 2B, and the emission spectra of EB-DNA(*c-myc* G4 DNA) in the absence and in presence of **1** and **2** was illustrated in Figure 2C and 2D.

As shown in **Figure 2A**, the electronic spectra of **1** in Tris-HCl buffer (10 mM Tris, 100 mM KCl, pH 7.4) exhibits a characteristic absorption at 278 nm, which can be attributed to intraligand (IL) charge transfer. The shoulder peak at 302 nm can be attributed to the ligand-to-metal charge transfer (LMCT) absorption. As for **2,** the characteristic IL and LMCT absorption appeared at 278 and 300nm, respectively. Besides, a weak absorption band was observed at 408 nm in the electronic spectra of **2**, which can be attributed to metal-to-ligand charge transfer (MLCT) absorption. Upon the addition of *c-myc* G4 DNA, obviously hypochromism was observed for both complexes. The hypochromism of **1** and **2** at IL absorption band were 20.7% and 26.2%, respectively.[18] These data indicated that both arene Ru(II) complexes bound to *c-myc* G4 DNA with high affinity, and the presence of the methyl group in the arene ligand contribute to increase the binding affinity.

As shown in **Figure 2C** and **2D**, the EB-DNA (*c-myc* G4 DNA) solution exhibits strong fluorescence in the range of 500 to 700 nm (excited at 350 nm), with the maximum at 600 nm.[19] When **1** or **2** was added to the solution, a noticeable decrease in the fluorescence intensity was observed, implying that **1** and **2** formed a competitive association with G4 DNA by replacing EB. At the [Ru]= 6 μM, the relative fluorescence strengths (I/I_0) of the solution in the presence of complexes **1** and **2** were 0.60 and 0.62, respectively. Complex **2** bind with *c-myc* G4 DNA more stronger than **1**, which were in agreement with the results of electronic spectra, indicating that both complexes exhibited a certain interaction with G-quadruplex DNA.

Isothermal Titration Calorimetry (ITC).

ITC experiments were carried out to further clarify the energetic basis of the interactions with *c-myc* G4 DNA. The ITC experiment curves were shown in **Figure 3**, and the experimental thermodynamic values were listed in **Table 1**.

ITC experiments afford the observed binding enthalpy, ΔH, and allowed the calculation of the entropy of binding ($\Delta G = \Delta H - T\Delta S$). The titration of complex **1** into buffer and *c-myc* G4 DNA solution provided plots of heat versus molar ratio. The titration

Table 1. Binding constants and experimental thermodynamic values at 25 °C for interactions of **1** and **2** with *c-myc* G4 DNA

Comp.	$K_1(M^{-1})$	$K_2(M^{-1})$	ΔH_1 (cal/mol)	ΔH_2 (cal/mol)	$T\Delta S_1$ (cal/mol)	$T\Delta S_2$ (cal/mol)	ΔG_1 (cal/mol)	ΔG_2 (cal/mol)
1	1.21×10^3	/	-5.5	/	1.6	/	-7.1	/
2	1.10×10^3	3.62×10^5	-5.7	-9.6.	1.3	3.2	-7.0	-12.8

plot strongly supports the proposition that **1** binds to *c-myc* G4 DNA in a one-site mode and completely saturates at a 1:1 stoichiometry. The binding constant calculated for **1** [K_1] is about 1.21×10^3 M^{-1}. As for **2,** a two-site mode was suggested and the saturated stoichiometry is 2:1. The binding constants calculated for **2** is [K_1]=1.10×10^3 M^{-1} and [K_2]=3.62×10^5 M^{-1}, respectively.[20] These results suggested that the methyl group in the arene ligand enhance the binding ability of arene Ru(II) complex to *c-myc* G4 DNA.

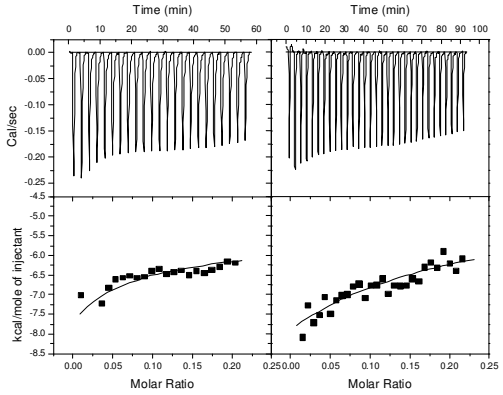

Fig. 3 ITC experimental curves at 25 °C for titration of **1** (left) and **2** (right) with *c-myc* G4 DNA. Results were converted to molar heat and plotted against the compound/DNA molar ratio. The line shows the fit to the results and gives the best-fit ΔH values for binding, [DNA] = 2 μM.

FRET Assay.

FRET (fluorescence resonance energy transfer) assay is often utilized to monitor the 3-to-5-end distance to investigate the interation of ligands with biomacromolecules.[21] FRET is a distance-dependent interaction between two dye molecules in

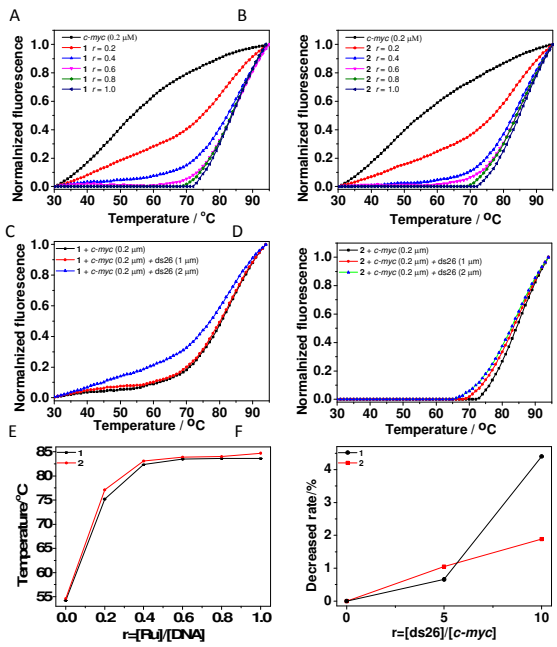

Fig. 4 FRET-melting curves obtained with *c-myc* G-quadruplex DNA (0.2 μM) alone (■) upon addition of **1** (A) and **2** (B). Competive FRET-melting curves obtained with *c-myc* G-quadruplex DNA (0.2 μM) and **1** (0.2 μM) (■) upon addition of ds26 DNA (C), for **2** (D). The increasing trend of *c-myc* melting upon the addition of **1** and **2** (E), r=[Ru]/[*c-myc*]=0, 0.2, 0.4, 0.6, 0.8 and 1.The selective binding affinity of **1** and **2** between *c-myc* G-quadruplex DNA and ds26 duplex DNA (F). Y-axis: the decreased rate of *c-myc* melting; X-axis: the concentration ratio of [ds26]/[*c-myc*]

which excitation is radiationlessly transferred from one dye (the donor 6-FAM) to the second dye (the acceptor TAMRA), due to spectral overlap. For further confirmed the binding ability of arene Ru(II) complex with *c-myc* G4 DNA, FRET melting assay was carried out to investigate the melting changes of **1** and **2** to *c-myc* G-quadruplex DNA. Furthermore, the competitive FRET assay also performed to confirm the selectivity of arene Ru(II) complexes between *c-myc* G-quadruplex DNA and ds26 duplex DNA. The results were shown in **Figure 4**.

As shown in **Figure 4A** and **4B**, upon the addition of **1** and **2,** the melting point of *c-myc* G4 DNA increased following the concentration of arene Ru(II) complexes. At *r*([Ru]/[DNA])=1.0, the melting point of *c-myc* G4 DNA reach to the maximum, and the ΔT_m for **1** and **2** is about 29.9 and 30.7 °C (**Figure 4E**), respectively. These results suggeted that arene Ru(II) complexes can stabilize the G-quadruplex formation, and **2** exhibits better stability than **1**, which is agreement with above experiments.[22]

Furthermore, the competitive FRET assay also performed to confirm the selectivity of arene Ru(II) complexes between *c-myc* G-quadruplex DNA and ds26 duplex DNA. In the FRET competitive experiments, it's observed that both arene Ru(II) complexes exhibit excellent selectivity to *c-myc* G-quadruplex DNA than ds26 duplex DNA. The melting point for *c-myc* G4 DNA in the presence of **1** and **2** is about 80.7 and 84.2 °C, respectively. In the presence of excess duplex ds26 DNA, the melting of *c-myc* G4 DNA undergo almost little obvious change (**Figure 4C** and **4D**). When *r*([ds26]/[*c-myc*]) =10, the ΔT_m for **1** and **2** is about 3.3 and 1.7 °C with a drop of less than 5%, respectively (**Figure 4F**). The results were in agreement with above experiments, indicated that this class of arene Ru(II) complexes could selectively bind with G-quadruplex DNA more strongly than duplex DNA.[23]

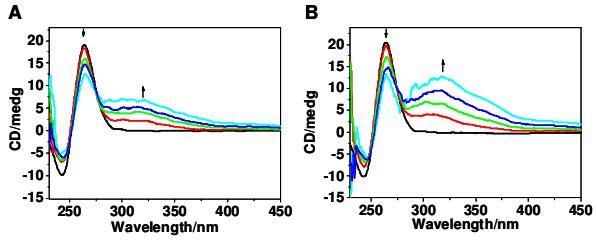

Fig. 5 CD titration spectra of *c-myc* G4 DNA (2 μM) at different concentrations of **1** (A) and **2** (B) ([Ru] =0, 0.667, 1.334, 2, 2.667 μM) in the incubation buffer.

Circular Dichroism(CD) Spectroscopy.

CD titration experiment was also carried out to investigate the conformation change of *c-myc* G4 DNA in the presence of arene Ru(II) complexes, and the results are shown in **Figure 5**.

Both arene Ru(II) complexes have no intrinsic CD signals because they are achiral. The CD spectra of *c-myc* G4 DNA in the incubation buffer exhibit a strong positive signal in the range of 250 – 300 nm with the maximum at 263 nm, in addition to a weak negative CD signal between 200 and 250 nm with the maximum at 245 nm.[24] The strength of CD signal decreased with the increasing concentration of the complexes. For 1, the strength of positive CD signal at 263 nm decreased by 35.8%, while the strength of the negative CD signal at 245nm decreased by 52.6%. It is worth noting that there are an apparent positive induced CD signal observed in the range of 300 - 400 nm, which has been consider as an admitted proof to indicate that the complex may bind to *c-myc* G-quadruplex DNA in groove binding mode.[21-25] The similar phenomenon was observed for **2**; the decrease in the strength of the positive CD signal at 263nm is 39.7% and the decrease in the strength of the negative CD signal at 245nm is 40.0%. Besides, there is a large induced CD signal appeared in the range of 290-400nm for **2**, either. These results indicated that arene Ru(II) complexes may bind to *c-myc* G-quadruplex DNA in groove binding mode, which complex **2** bind to *c-myc* G-quadruplex DNA stronger than **1.**

Molecular Docking.

In order to find the most favorable orientation of these Ru(II) complexes with the *c-myc* G-quadruplex DNA, molecular docking study of Ru(II) complexes was performed using the Lamarckian genetic algorithm local search method with AutoDock4.2.[26] The crystallographic structure of c-*myc* G-quadruplex DNA was downloaded from the Protein Data Bank (PDB ID: 2L7V). Only chain A was maintained by removing other subunits. AutoDock tools were utilized to assign Gasteiger charge and other parameters. The grid box was centered on the c-*myc* G-quadruplex DNA with (x,y,z)=(2.579 -0.627 -4.749) and its size was set to 126×126×126 points. 50 separate dockings were performed with maximum of energy evaluations to 2.5×10^7. The conformation corresponding to the most cluster members and

the lowest binding free energy was selected as the most probable binding conformation.

According to the calculation results, it's found that both complexes can insert into the groove of *c-myc* G4 DNA, which formed by base pairs A6~G9 and G21~A25. Meanwhile, the H atom of N atom in imidazole ring of both complexes can form a hydrogen bond with G8 guanine in *c-myc* G4 DNA (**Figure 6A**).

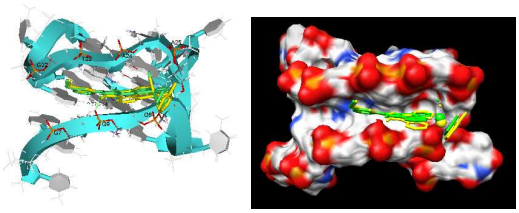

A B

Fig. 6 The binding site (A) and binding mode (B) of complex **1** and **2** with *c-myc* G4 DNA caculated by molecular docking.

As shown in Figure 6B, complexes **1** and **2** interact with *c-myc* G4 DNA via a typical groove binding mode. These data were consistent with CD spectra, indicated that arene Ru(II) complex might as a groove binder to *c-myc* G4 DNA.

^{1}H NMR Analysis.

^{1}H NMR analysis was a common method to evestigate the binding mode of compounds interact with biomacromolecules.[27] To futher confirm the interaction of both arene Ru(II) complexes bind to *c-myc* G4 DNA, ^{1}H NMR analysis was used to monitor the binding mode and binding site of **1** and **2** with *c-myc* G4 DNA. As shown in Figure 6, the aromatic regions proton resonances located between 7.0 and 9.0 indicate the formation of *c-myc* G-quadruplex structure.[28] The proton at 8.56 (s, 1H) and 8.46 (s, 1H) ppm was attributed to A15 which was a proton of Me in aromatic region and a series of signals at 7.74, 7.10 and 7.52, 7.41 ppm were affiliated to the protons on the A24 and A25, respectively. Besides, the protons of G16, G17, G21 and G22 were affiliated at 8.10, 7.86, 7.89 and 7.65 ppm, respectively.

However, upon the increasing of **1** and **2**, the signals of A15, A24, A25, G16, G17, G21 and G22 changed to be weaken and broaden notably, the signals followed with the addition of **2** decreased more distinct than **1** at the same concentration.[27] These reslults indicated that **2** bind to *c-myc* G-quadruplex DNA in a groove binding mode by interacted with T14~G17 and G21~A25 stronger than **1**, which were in agreement with molecular docking calculation.

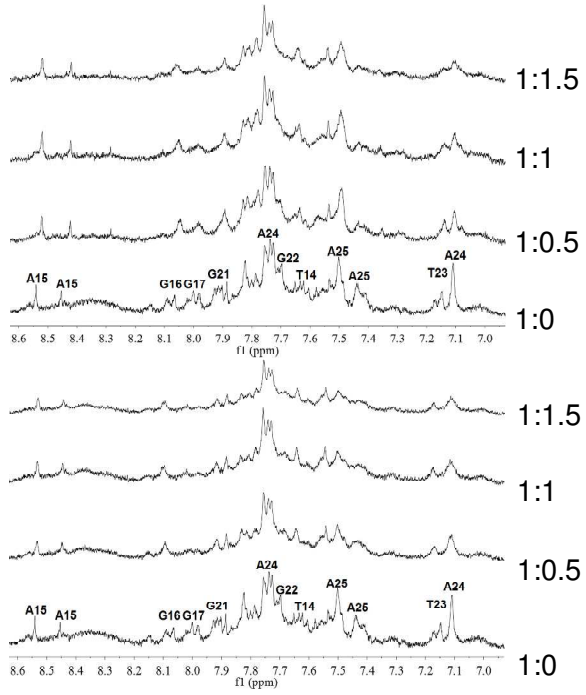

Fig. 7 The ^{1}H NMR spectra of *c-myc* in aromatc regions treated with different concentration of **1** (A) and **2** (B). [*c-myc*]=100 μM, [Ru]=0, 50, 100 and 150μM.

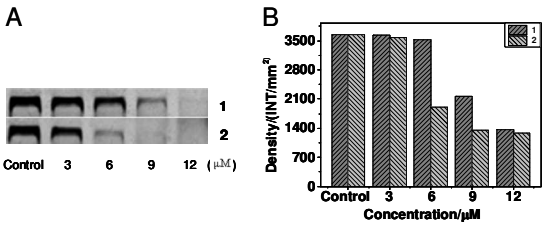

Fig. 8 (A) Effect of complex **1** and **2** on the PCR-stop assay with *c-myc* G4 DNA. [Ru]=0, 3, 6, 9, and 12 μM, [*c-myc*]=10 pM. (B) The replication blocking of PCR products obtained for different complex concentrations.

PCR-stop Assay.

PCR-stop assay was utilized to evaluate the inhibitory activity of the complexes against Taq polymerase by stabilizing the *c-myc* G-quadruplex conformation. As shown in **Figure 7**, it's observed a notable decrease in the amounts of PCR products as a result of the interaction between arene Ru(II) complexes and *c-myc* G-quadruplex DNA. Interestingly, the two complexes showed different inhibitory effects.[29] The minimum concentration of complex **2** (6 μM) necessary for effective interaction with *c-myc* G-quadruplex DNAwas significantly lower than that for complex **1** (9 μM). Complex **2** have a stronger inhibitory effect on the replication of *c-myc* than complex **1**. And comparison with the interaction of telomeric G-quadruplex DNA with some ruthenium(II) polypyridyl complexes ($[Ru(bpy)_2(ptpn)]^{2+}$ $[Ru(phen)_2(ptpn)]^{2+}$), which can promote the the formation and stabilization of the human telomeric G-quadruplex DNA to decrease the PCR products.[5c] This comparison was further indicated that this class of arene Ru(II) complexes can bind to and stable *c-myc* G-quadruplex DNA to decrease the replication.

Conclusions

In summary, two arene Ru(II) complexes coordinated by 2-(3-methoxyphenyl)imidazo[4,5*f*][1,10]phenanthroline were prepared and the crystal structure of both complexes gave a typical "piano stool" conformation. The evaluation of *in vitro* anticancer activities revealed that these synthetic Ru(II) complexes exhibited great selectivity between human cancer and normal cells, by comparing with the ligand *m*-MOPIP. Furthermore, the

investigations by spectroscopy, melting point experiments, ITC, and molecular docking methods demonstrated that these arene Ru(II) complexes exhibit excellent binding affinity to *c-myc* G4 DNA in groove binding mode, which was further confirmed by the ^{1}H NMR analysis. Finally, the replication of *c-myc* oncogene was effectively inhibited by the complexes *in vitro*. Taken together, these results suggest that arene Ru(II) complexes display application potential as small molecule inhibitors of *c-myc* G4 DNA.

Experimental Section

Reagents and Materials.

All reagents were used as purchased from commercial suppliers without further purification. Solvents were dried and purified by conventional methods prior to use. Ruthenium (Ru) chloride hydrate was obtained from Mitsuwa Chemicals. 1,10-Phenanthroline monohydrate, 1,3-cyclohexadiene, 1-methyl-1,4-cyclohexadiene and 3-methoxybenzaldehyde were purchased from Aladdin. 1,10-phenanthroline-5,6-dione: The compound was prepared by using the similar method reported the literatures.[30] The ligand 2-(3-methoxyphenyl)imidazo[4,5*f*][1,10]phenanthroline (*m*-MOPIP) was prepared by using the similar method as literatures,[31] Binuclear arene Ru(II) complexes: The binuclear arene Ru(II) complexes $[(C_6H_6)RuCl_2]_2$ and $[(C_6H_5Me)RuCl_2]_2$ were prepared according to literature. [32] All the chemicals including solvents were obtained from commercial vendors and used as received. *c-myc* G-quadruplex DNA (5'-TGGGGAGGGTGGGGA GGGTGGGGAAGG-3') and the fluorescent labeled oligonucleotide, *c-myc* G-quadruplex DNA (5'-FAM-TGGGGAGGGTGGGGAGGGTGGGGAAGG-TAMRA-3', FAM: carboxyfluorescein,TAMRA: 6-carboxytetramethylrhodamine) and ds26 duplex DNA were purchased from Sangon Biotech (Shanghai) Co., Ltd. and formed a G-quadruplex conformation by renaturation at 4˚C for 24 h after 90℃ denaturation for 5 min as literature.[28] All aqueous solutions were prepared with doubly distilled water. The Tris-HCl buffer is consisting of Tris (10 mM) and KCl (100 mM), and the pH value was adjusted to 7.4 by HCl (0.1 mol), which was applied to UV titration, fluorescence quenching, thermal denaturation, CD spectra, ITC and PCR-stop.

Instruments.

The arene Ru(II) complexes were synthesized by Anton Paar GmbH monowave 300 microwave reactor. The ^{1}H NMR, ^{13}C NMR and ^{1}H ^{1}H COSY spectra were recorded in DMSO-d^6 on BrukerDRX2500 spectrometer operating at room temperature. The electronic absorption spectra were recorded on a Shimadzu UV-2550 Spectrophotometer, the steady-state emission spectra were recorded on a RF-5301 Fluorescence Spectrophotometer, and the CD spectra were recorded on Jasco J810 Circular Dichrosim (CD) Spectrophotometer. ITC experiments were recorded on a American TA NANO ITC and PCR-stop assay were operated on AlphaSC Thermal Cycler. Molecular docking data were calculated by using Addsol, Autogrid and Auto Tors tool of the software. The X-ray intensity data (0.40 mm × 0.20 mm × 0.10 mm) were collected at 293(2) K on a Bruker SMART APEX 2K CCD-based X-ray diffractometer equipped with a graphite-monochromated MoKα radiation (λ=0.71073 Å). The collected frames were proessed with the software SHELXTL with 2001 Bruker Analytical X-ray Solutions.

Synthesis and characterization

Synthesis of $[(\eta^6\text{-}C_6H_6)Ru(m\text{-MOPIP})Cl]Cl\cdot 2H_2O$ (1). The arene Ru(II) complex **1** was synthesized according to literature,[33] but with some modification. In general, a mixture of $[(C_6H_6)RuCl_2]_2$ (0.035 mmol, 17.5 mg), *m*-MOPIP (0.07 mmol, 15.4 mg) and dichlormethane (7 mL) dissolved in SiC vessel under the protection of N_2 atomosphere, and then heated for 30 min under the irradiation of microwave at 60 ˚C. After the solvent was evaporated, the mixture was dissolved in methanol, and filtered to obtain a yellow crude product. Yield: 88.2%. ESI-MS (in MeOH, *m/z*): 541.1, ($[M\text{-}Cl]^+$). ^{1}H NMR (500MHz, DMSO-d^6, δ/ppm) 9.96 (d, 1H of N4), 9.72 (s, 2H of C14 and C17), 9.14 (s, 2H of C12 and C19), 8.16 (s, 2H of C13 and C18), 8.09 (s, 1H of C7), 8.02 (d, 1H of C5), 7.49 (t, 1H of C4), 7.10 (d, 1H of C3), 6.35 (s, 6H of C21~C26), 3.93 (s, 3H of C1). ^{13}C NMR (126 MHz, DMSO-d^6, δ/ppm): 160.2 (s, C8), 154.5 (s, C9 and C10), 153.1 (s, C14, C15, C16 and C17), 143.6 (s, C11 and C20), 133.7 (s, C10 and C18), 131.7 (s, C12 and C19), 119.6 (s, C6), 116.8 (s, C3, C4, C5 and C7), 112.2 (s, C2), 87.3 (s, C21~C26), 56.1 (s, C1).

Synthesis of $[(\eta^6\text{-}MeC_6H_5)Ru(m\text{-MOPIP})Cl]Cl\cdot 2H_2O$ (2). 2 was prepared in a similar method to that of above, but with $[(C_6H_5CH_3)RuCl_2]_2$ (0.035 mmol, 18.5 mg) and *m*-MOPIP (0.07 mmol, 15.4 mg). Yield: 90.3%. ESI-MS (in MeOH, *m/z*) : 555.1, ($[M\text{-}Cl]^+$). ^{1}H NMR (500MHz, DMSO-d^6, δ/ppm), 9.97 (d, 1H of N4), 9.73 (s, 2H of C14 and C17), 9.14 (s, 2H of C12 and C19), 8.17 (s, 2H of C13 and C18), 8.09 (s, 1H of C7), 8.03 (d, 1H of C5), 7.50 (t, 1H of C4), 7.10 (d, J = 8.2, 2.1 Hz, 1H of C3), 6.45 (t, 2H of C22 and C24), 6.10 (d, 2H of C21 and C25), 5.91 (t, 1H of C23), 3.93 (s, 3H of C1), 2.30 (s, 3H of C27). ^{13}C NMR (126 MHz, DMSO-d^6, δ/ppm) : 160.2 (s, C8), 154.3 (s, C9 and C10), 153.1 (s, C14, C15, C16 and C17), 143.8 (s, C11 and C20), 131.1 (s, C10 and C18), 130.7 (s, C12 and C19), 119.6 (s, C6), 116.9 (s, C3 , C4, C5 and C7), 112.2 (s, C2), 105.9 (s, C26), 90.4 (s, C22 and C24), 83.5 (s, C21 and C26), 80.4 (s, C23), 56.1 (s, C1), 19.3 (s, C27).

X-ray single crystal diffraction.

The crystal suitable for X-ray diffraction was obtained by recrystalization after filter in DMF solution by adding petroleum ether into the solution slowly through solvent volatilization, and then the solution was keep in dark for seven days at room temperature to give a yellow block shaped crystals. The X-ray intensity data for two complexes were collected at X-ray diffractometer equipped with a graphite-monochromated MoKα radiation (λ=0.71073 Å) by using a ω scan mode ($0.99° < \theta < 27.12°$).

Cell Lines and Cell Culture.

HepG2 hepatocellular carcinoma and LO2 normal human liver cells were purchased from American Type Culture Collection (ATCC, Manassas, VA), and maintained in DMEM medium supplemented with fetal bovine serum (10%), penicillin (100 units/ml) and streptomycin (50 units/ml) at 37℃ in CO_2 incubator (95% relative humidity, 5% CO_2).

MTT Assay.

All complexes were dissolved in DMSO with stock solution at 10 mg/ml. Cell viability was determined by measuring the ability of cells to transform MTT to a purple formazan dye.[34] Cells were seeded in 96-well tissue culture plates (3×10^3 cells/well) for 24 h. The cells were then incubated with the tested compounds at different concentrations for 72 h. After incubation, 20 μl/well of MTT solution (5 mg/ml phosphate buffered saline) was added and incubated for 5 h. The medium was aspirated and replaced with DMSO (150 μl/wel) to dissolve the formazan salt. The absorbance intensity, which reflects the cell growth condition, was measured at 570 nm using a microplate spectrophotometer (Versamax).

UV Titration.

UV-vis absorption spectra were recorded on a Shimadzu UV-2550 spectrophotometer using 1 cm path length quartz cuvettes (3 mL). The absorption titration of the Ru(II) complex in Tris-HCl buffer was performed by using a fixed complex concentration to which increments of the DNA stock solution were added. The concentration of the complex solution was 20 μM and *c-myc* G4 DNA was added by degrees. Complex-DNA solutions were allowed to incubate for 3 min before the absorption spectra were recorded.[35]

Fluorescence Spectroscopy.

Fluorescence spectroscopy measurements were performed on a RF-5301 Fluorescence Spectrophotometer using a 1 cm path length quartz cell. Fluorescence quenching of EB+*c-myc* DNA system can be used for a compound having an affinity to DNA in spite of its binding mode, and only measures the ability of the compound to affect the EB fluorescence intensities in the EB+*c-myc* DNA system.[36]

Isothermal Titration Calorimetry.

Binding of various small molecules was assessed by isothermal titration calorimetry on a thermostated Micro Cal VP-ITC system. *c-myc* G4 DNA dissolved in Tris-HCl KCl buffer were diluted directly into complex buffer if the added volume would comprise less than 1% of the final volume. Otherwise, *c-myc* G4 DNA solutions were dried on a Speedvac and DNA dissolved in complex buffer. All solutions were degassed prior to use. Data were analyzed by Origin 8.5. (MicroCal). Heats of dilution were subtracted from all data before fitting. Each dilution heat was determined in an independent control experiment by injecting the complex into buffer. These heats were much smaller than the heats of binding. Data analysis requires a binding model, and fitting returns values for the binding constant K, squares ΔH of binding, ΔS of binding, and the binding stoichiometry n. The Gibbs free energy change, ΔG, and the entropy change, ΔS, were calculated using the equation ΔG=-RTln$K$= ΔH-$T\Delta S$.[37]

FRET melting and Competitive FRET assays.

The fluorescent labeled oligonucleotide, *c-myc* G-quadruplex DNA (5'-FAM-TGGGGAGGGTGGGGAGGGTGGGGAAGG-TAMRA-3', FAM: carboxyfluorescein,TAMRA: 6-carboxytetramethylrhodamine) used as the FRET probes was diluted in Tris-HCl buffer and then annealed by being heated to 92°C for 5 min, followed by slowly cooling to room temperature.[21] ds26 duplex DNA was a competive binder to evaluate the selectivel binding ability of arene Ru(II) complex with *c-myc* G4 DNA Fluorescence melting curves were determined with a Bio-Radi Q5 realtime PCR detection system, by using a total reaction volume of 25 mL,with labeled oligonucleotide (1 μM) and different concentrations of complexes in Tris-HCl buffer.[25] A constant temperature was maintained for 30 s priortoea chreading to ensure a stable value. Final nalysis of the data was carried out by using Origin7.5(Origin Lab Corp.).

Circular Dichroism.

CD spectra were recorded on a Jasco J810 Circular Dichrosim (CD) Spectrophotometer with a thermoelectrically controlled cell holder. The cell path length was 1 cm. CD spectra were recorded in the range of 230–600 nm in 0.5 nm increments with an averaging time of 0.5 s .[24]

Molecular Docking.

Automated docking studies were per-formed with three different docking algorithms, AutoDock 3.0 ('Lamarckian' genetic algorithm),[38] FlexX 1.10 (incremental construction algorithm,[39] as implemented in Sybyl 6.8), and GOLD 1.2 ('Darwinian' genetic algorithm).[40] As scoring is a very important second aspect of automated docking method-ologies, it was decided to investigate the effect of rescoring: the process of reprioritization of docking solutions (primarily ranked by the 'native' scoring function implemented in the docking program) with an additional stand-alone scoring function.

^{1}H NMR Assay.

^{1}H NMR spectra was tested on BrukerDRX2500 spectrometer. All titration experiments were performed at 30 °C in 90% H_2O/10% D_2O solution containing 150 mM KCl, 25 mM KH_2PO_4, and 1 mM EDTA (pH7.0). A standard echo pulse sequence with a maximum excitation centered at 12.0 ppm was used for water suppression. And spectra were recorded at 300 K utilizing a standard jump, thirty-two scans were acquired for each spectrum with a relaxation delay of 2 s. ^{1}H NMR results were processed and analyzed using the FELIX program. [41]

PCR-stop Assay.

The PCR-stop assay was performed by using a modied protocol

of the previously reported method.[31] The reactions (40 μL) were performed in 1×PCR buffer, containing each pair of *c-myc* G-quadruplex DNA (10 pM), deoxy nucleotide triphosphate (0.16mM), Taqpolymerase (2.5U), and increasing concentrations of the compound (0-250μM). The reaction mixtures were incubation in athermocycler under the following cycling conditions: 94°C for 3 min followed by 30 cycles at 94 °C for 30 s, 58 °C for 30 s, 72 °C for 30 s. Amplified products were resolved on 15% nondenaturing polyacrylamide gels in 1×TBE and silver stained.

Statistical Analysis

Experiments were carried out at least in triplicate and results were expressed as mean ± SD. Statistical analysis was performed using SPSS statistical program version 13 (SPSS Inc., Chicago, IL). Difference with $P < 0.05$ (*) or $P < 0.01$ (**) was considered statistically significant.

Acknowledgements

This work was supported by Natural Science Foundation of China and Guangdong Province, Key Project of Science and Technology Department of Guangdong Province, the Fundamental Research Funds for the Central Universities, Program for New Century Excellent Talents in University, and the Planned Project of Science and Technology Foundatiuon of Guangzhou.

Notes and references

a School of Pharmacy, Guangdong Pharmaceutical University, Guangzhou, 510006, P.R. China. E-mail: wenjiemei@126.com,

b Department of Chemistry, Jinan University, Guangzhou, 510632, P.R. China. E-mail: tzhwj@jnu.edu.cn

c School of Pharmaceutical Sciences, Guangzhou Medical University, Guangzhou, 510182, P.R. China

 # Authors contributed equally to the work.

† Electronic Supplementary Information (ESI) available: Experimental details for microwave-assisted synthesis of arene ruthenium(II) complexes (**1** and **2**) and crystallographic data for the complexes. See DOI: 10.1039/b000000x/

1 (a) Calado, D. P.; Sasaki, Y.; Godinho, S. A.; Pellerin, A.; Köchert, K.; Sleckman, B. P.; Alborán, I. M.; Janz, M.; Rodig, S.; Rajewsky, K. *Nat. Immunol.,* 2012, **13**, 1092-1100; (b) Tsai, Y. C.; Qi, H.; Lin, C. P.; Lin, R. K.; Kerrigan, J. E.; Rzuczek, S. G.; LaVoie, E. J.; Rice, J. E.; Pilch, D. S.; Lyu, Y. L.; Liu, L. F. *J Biol Chem.,* 2009, **284**, 22535-22543; (c) Zhang, J. Y.; Tao, L. Y.; Liang, Y. J.; Yan, Y. Y.; Dai, C. L.; Xia, X. K.; She, Z. G.; Lin, Y. C.; Fu, L. W. *Cell Cycle.,* 2009, **8**, 2444-2450; (d) Delmore, J. E.; Issa, G. C.; Lemieux, M. E.; Rahl, P. B.; Shi, J.; Jacobs, H. M.; Kastritis, E.; Gilpatrick, T.; Paranal, R. M.; Qi, J.; Chesi, M.; Schinzel, A. C.; McKeown, M. R.; Heffernan, T. P.; Vakoc, C. R.; Bergsagel, P. L.; Ghobrial, I. M.; Richardson, P. G.; Young, R. A.; Hahn, W. C.; Anderson, K. C.; Kung, A. L.; Bradner, J. E. *Cell*, 2011,**146**, 904-917.

2 (a)Mergny, J. L.; Helene, C. *Nat. Med.,* 1998, **4**, 1366-1367; (b) Wei, C.; Jia, G.; Yuan, J.; Feng, Z.; Li, C. *Biochemistry,* 2006, **45**, 6681-6691; (c) Boddupally, P. V.; Hahn, S.; Beman, C.; De, B.; Brooks, T. A.; Gokhale, V.; Hurley, L. H. *J. Med. Chem.,* 2012, **55**, 6076-6086; (d) Brooks, T. A.; Hurley, L. H. *Genes Cancer.,* 2010, **1**, 641-649.

3 Mei, W. J.; Wei X. Y.; Liu, Y. J.; Wang, B. *Trans. Met. Chem.,* 2008, **33**, 907-910.

4 Zimbron, J. M.; Sardo, A.; Heinisch, T.; Wohlschlager, T.; Gradinaru, J.; Massa, C.; Schirmer, T.; Creus, M.; Ward, T. R. *Chemistry*, 2010, **16**, 12883-12889.

5 (a) Liao, G. L.; Chen, X.; Ji, L. N.; Chao, H. *Chem. Commun (Camb).,* 2012, **48**, 10781-10783; (b) Yao, J. L.; Gao, X.; Sun, W.; Fan, X. Z.; Shi, S.; Yao, T. M. *Inorg Chem.,* 2012, **51**, 12591-12593; (c) Chen, X.; Wu, J. H.; Lai, Y. W.; Zhao, R.; Chao, H.; Ji, L. N. *Dalton Trans.,* 2013, **42**, 4386-4397; (d) Wilson, T.; Costa, P. J.; Felix, V.; Williamson, M. P.; Thomas, J. A. *J. Med. Chem.,* 2013 in press; (e) Shi, S.; Zhao, J.; Gao, X.; Lv, C.; Yang, L.; Hao, J.; Huang, H.; Yao, J.; Sun, W.; Yao, T.; Ji, L. N. *Dalton Trans.,* 2012, **41**, 5789-5793.

6 Wu, K.; Liu, S.; Luo, Q.; Hu, W.; Li, X.; Wang, F.; Zheng, R.; Cui, J.; Sadler, P. J.; Xiang, J.; Shi, Q.; Xiong, S. *Inorg. Chem.,* 2013, **52**, 11332-11342.

7 (a) Singh, A. K.; Pandey, D. S.; Xu, Q.; Braunstein, P. *Coord. Chem. Rev.,* 2013, In Press; (b) Liu, H. K.; Sadler, P. J. Acc. *Chem. Res.,* 2011, *44*, 349; (c) Yan, Y. K.; Melchart, M.; Habtemariam, A.; Sadler, P. J. *Chem. Commun.*, 2005, 4764-4776; (d) Pizarro, A. M.; Sadler, P. J. *Biochimie.* 2009, **91**, 1198-1211; (e) Suss-Fink, G. *Dalton Trans.,* 2010, **39**, 1673-1688; (f) Barry N. P. E.; Karim N. H. A.; Vilar R.; Therrien B. *Dalton Trans.*, 2009, 10717-10719; (g) Gianferrara T.; Bratsos I.; Iengo E.; Milani B.; Oštrić A.; Spagnul C.; Zangrandob E.; Alessio E. *Dalton Trans.*, 2009, 10742-10756.

8 (a) Scolaro, C.; Bergamo, A.; Brescacin, L.; Delfino, R.; Cocchietto, M.; Laurenczy, G.; Geldbach, T. J.; Sava, G.; Dyson, P. J. *J. Med. Chem.,* 2005, **48**, 4161-4171; (b) Martinez, A.; Rajapakse, C. S.; Sanchez-Delgado, R. A.; Varela-Ramirez, A.; Lema, C.; Aguilera, R. J. *J. Inorg. Biochem.,* 2010, **104**, 967-977; (c)Vajpayee, V.; Yang, Y. J.; Kang, S. C.; Kim, H.; Kim, I. S.; Wang, M.; Stang, P. J.; Chi, K. W. *Chem. Commun.,* 2011, **47**, 5184-5186; (d) Kisova, A.; Zerzankova, L.; Habtemariam, A.; Sadler, P. J.; Brabec, V.; Kasparkova, *J. Mol. Pharm.* 2011, **8**, 949-956; (e) Ratanaphan, A.; Temboot, P.; Dyson, P. J. *Chem. Biodivers.,* 2010, **7**, 1290-1302; (f) Chatterjee, S.; Kundu, S.; Bhattacharyya, A.; Hartinger, C. G.; Dyson, P. J. *J. Biol. Inorg. Chem.,* 2008, **13**, 1149-1155; (g) Martinez, A.; Rajapakse, C.S.K.; Sánchez-Delgado, R. A.; Varela-Ramirez, A.; Lema, C.; Aguilera, R. J. *J. Inorg. Biochem.*2010, **104**, 967-977.

9 Bonfili, L.; Pettinari, R.; Cuccioloni, M.; Cecarini, V.; Mozzicafreddo, M.; Angeletti, M.; Lupidi, G.; Marchetti, F.; Pettinari, C.; Eleuteri, A. M. *Chem. Med. Chem.,* 2012, **7**, 2010-2020.

10 Zhang, G.; Wu, C.; Ye, H.; Yan, H.; Wang, X.; *J. Nanobiotechnology.* 2011, **9**, 6.

11 Wu, Q.; Fan, C. D.; Chen, T. F.; Liu, C. R.; Mei, W. J.; Chen, S. D.; Wang, B. G.; Chen, Y. Y.; Zheng, W. J. *Eur, J. Med. Chem.,* 2013, **63**, 57-63.

12 Caruso, F.; Rossi, M.; Benson, A.; Opazo. C.; Freedman, D.; Monti, E.; Gariboldi, M. B.; Shaulky, J.; Marchetti, F.; Pettinari, R.; Pettinari, C. *J. Med. Chem.,* 2012, **55**, 1072-1081.

13 (a) Roux-Dosseto, M.; Romain, S.; Dussault, N.; Desideri, C.; Piana, L.; Bonnier, P.; Tubiana, N.; Martin, P. M. *Eur. J. Cancer.,* 1992, **28**, 1597-1600; (b) Sharrard, R. M.; Royds, J. A.; Rogers, S.; Shorthouse, A. J. *Br. J. Cancer.,* 1992, **65**, 667-672.

14 Gubala, V.; Betancourt, J .E.; Rivera, J. M. *Org. Lett.,* 2004, **6**, 4735-4738.

15 Lin, C. P.; Liu, J. D.; Chow, J. M.; Liu, C. R.; Liu, H. E. *Anticancer Drugs.,* 2007, **18**, 161-170.

16 De Rache, A.; Kejnovska, I.; Vorlickova, M.; Buess-Herman, C. *Chemistry,* 2012, **18**, 4392-4400.

17 (a)Poteet, S. A.; Majewski, M. B.; Breitbach, Z. S.; Griffith, C .A.; Singh, S.; Armstrong, D. W.; Wolf , M. O.; Macdonnell, F. M. *J. Am. Chem. Soc.,* 2013, **135**, 2419-2422; (b) Vock, C. A.; Scolaro, C.; Phillips, A. D.; Scopelliti, R.; Sava, G.; Dyson, P. J. *J. Med. Chem.,* 2006, **49**, 5552-5561.

18 (a) Zhu, J. D.; Sun, X. P,.; Wang, F. *Biochim. Biophys. Acta.,* 1991, **1089**, 158-166; (b) Vaishnavi, E.; Renganathan, R. *Bull. Mater. Sci.*, 2012, **15**, 1173-1179.

19 Li, L. Y.; Jia, H. N.; Yu, H .J.; Du, K. J.; Lin, Q. T.; Qiu, K. Q.; Chao, H.; Ji, L. N. *J. Inorg. Biochem.,* 2012, **113**, 31-39.

20 Mergny, J. L.; Maurizot, J. C. *Chem. Bio. Chem.,* 2001, **2**, 124-134.

21 Kieltyka, R.; Englebienne, P.; Fakhoury, J.; Autexier, C.; Moitessier, N.; Sleiman, H. F. *J. Am. Chem. Soc.,* 2008, **130**, 10040-10041.

22 (a) Cian, A. D.; DeLemos, E.; Mergny, J. L.; Teulade-Fichou, M. P.; Monchaud, D. *J. Am. Chem. Soc*., 2007, **129**, 1856-1857; (b) Peng, D.; Tan, J. H.; Chen, S. B.; Ou, T. M.; Gu, L. Q.; Huang, Z. S. *Bioorg. Med. Chem.,* 2010, **18**, 8235-8242.

23 Ossipov, D.; Pradeepkumar, P. I.; Holmer, M,.; Chattopadhyaya, J. *J. Am. Chem. Soc.,* 2001, **123**, 3551-3562;

24 Maheswari,, P. U.; Rajendiran, V.; Palaniandavar, M.; Parthasarathi, R.; Subramanian, V. *J. Inorg. Biochem.,* 2006, **100**, 3-17.

25 Kitchen, D. B.; Decornez, H.; Furr, J. R.; Bajorath, J. *Nat. Rev. Drug Discov.,* 2004, **3**, 935-949.

26 (a)Haider, S. M.; Neidle, S.; Parkinson, G. N. *Biochimie,* 2011, **93**, 1239-1251; (b) Morris, G. M.; Huey, R.; Lindstrom, W.; Sanner, M. F.; Belew, R. K.; Goodsell, D. S.; Olson, A. J. *J. Comput. Chem.* 2009, **30**, 2785 –2791.

27 Ou, T. M.; Lu, Y. J.; Zhang, C.; Huang, Z. S.; Wang, X. D.; Tan, J. H.; Chen, Y.; Ma, D. L.; Wong, K. Y.; Tang, J.C.; Chan, A. S.; Gu, L. Q. *J. Med. Chem.,* 2007. **50**, 1465-1474.

28 (a) Chan, D. S.; Yang, H.; Kwan, M. H.; Cheng, Z.; Lee, P.; Bai, L. P.; Jiang, Z. H.; Wong, C. Y.; Fong, W. F.; Leung, C. H.; Ma, D. L. *Biochimie*., 2011, **93**, 1055-1064; (b) Ambrus, A.; Chen, D.; Dai, J.; Jones, R. A.; Yang, D. *Biochemistry,* 2005, **44**, 2048-2058.

29 Rajendiran, V.; Murali, M.; Suresh, E.; Sinha, S.; Somasundaram, K.; Palaniandavar, M. *Dalton Trans.,* 2008, 148-163.

30 Zhang, Z.; Wang, Q.; Wu, Q.; Hu, X. Y.; Wang, C. X.; Mei, W. J.; Tao, Y. Y.; Wu, W. L.; Zheng, W. J. *Chem. J. Chin. Univ.*, 2012. **33**, 2441-2446.

31 Therrien, B. *Coord. Chem. Rev.,* 2009, **253**, 493-519.

32 Wu, Q.; Wu, J.; Mei, W. J.; Yao, J. H.; Wu, W. L.; Chen, Y. H.; Tao, Y. Y. *Chinese J. Org. Chem.,* 2013, **33**, 2022-2027.

33 Chen, T.; Wong, Y.S. *Biomed. Pharmacother.* 2009, **63**, 105-113.

34 Mei, W. J.; Liu, J.; Zheng, K. C.; Lin, L. J.; Chao, H.; Li, A. X.; Yun, F. C.; Ji, L. N. *Dalton Trans.,* 2003, 1352-1359.

35 Vaidyanathan, V. G.; Nair, B. U. *J. Inorg. Biochem.,* 2002, **91**, 405-412.

36 Andersson, J.; Fornander, L. H.; Abrahamsson, M.; Tuite, E.; Nordell, P.; Lincoln, P. *Inorg. Chem.,* 2013, **52**, 1151-1159.

37 Morris, G. M.; Goodsell, D. S.; Halliday, R. S.; Huey, R.; Hart, W. E.; Belew, R. K.; Olson, J. *J. Comput. Chem.,* 1998, **19**, 1639-1662.

38 Rarey, M.; Kramer, B.; Lengauer, T.; Klebe, G. *J. Mol. Biol.,* 1996, **261**, 470-489.

39 Jones, G.; Willett, P.; Glen, R. C.; Leach, A. R.; Taylor, R. *J. Mol. Biol.,* 1997, **267**, 727-748.

40 Sun H. X.; Xiang J. F.; Gai W.; Liu Y.; Guan A. J.; Yang Q. F.; Li Q.; Shang Q.; Su H.; Tang Y. L.; Xu G. Z. *Chem. Commun.,* 2013, **49**, 4510-4512.

Tables and Figures

Fig.1 The molecular structure of the lattice and the atom numbers of **1** and **2.**

Fig.2 The study of interaction between arene Ru(II) **1** and **2** with *c-myc* G4 DNA by Spectroscopic methods. The electronic spectra of arene Ru(II) complex **1** (A) and **2** (B) in the absence and presence of *c-myc* G4 DNA, [Ru] = 20 μM. Emission spectra of EB and *c-myc* G4 DNA in the incubation buffer in the absence and presence of **1** (C) and **2** (D), [EB] = 16 μM, [DNA] = 2 μM.

Fig. 3 ITC experimental curves at 25 °C for titration of **1** (left) and **2** (right) with *c-myc* G4 DNA. Results were converted to molar heat and plotted against the compound/DNA molar ratio. The line shows the fit to the results and gives the best-fit ΔH values for binding, [DNA] = 2 μM.

Fig. 4 FRET-melting curves obtained with *c-myc* G-quadruplex DNA (0.2 μM) alone (■) upon addition of **1** (A) and **2** (B). Competive FRET-melting curves obtained with *c-myc* G-quadruplex DNA (0.2 μM) and **1** (0.2 μM) (■) upon addition of ds26 DNA (C), for **2** (D). The increasing trend of *c-myc* melting upon the addition of **1** and **2** (E), r=[Ru]/[*c-myc*]=0, 0.2, 0.4, 0.6, 0.8 and 1.The selective binding affinity of **1** and **2** between *c-myc* G-quadruplex DNA and ds26 duplex DNA (F). Y-axis: the decreased rate of *c-myc* melting; X-axis: the concentration ratio of [ds26]/[*c-myc*].

Fig. 5 CD titration spectra of *c-myc* G4 DNA (2 μM) at different concentrations of **1** (A) and **2** (B) in the incubation buffer.

Fig. 6 The binding site (A) and binding mode (B) of complex 1 and 2 with *c-myc* G4 DNA caculated by molecular docking

Fig. 7 The ^{1}H NMR spectra of *c-myc* treated with different concentration of **1** (A) and **2** (B). [*c-myc*]=100 μM, [Ru]=0, 50, 100 and 150μM.

Fig. 8 (A) Effect of complex **1** and **2** on the PCR-stop assay with *c-myc* G4 DNA. [Ru]=0, 3, 6, 9, and 12 μM, [*c-myc*]=10 pM. (B) The replication blocking of PCR products obtained for different complex concentrations.

Table 1. Inhibitory effect of arene Ru(II) complexes on human liver cancer and normal cells.

Table 2. Binding constants and experimental thermodynamic values at 25 ℃ for interactions of **1** and **2** with *c-myc* G4 DNA

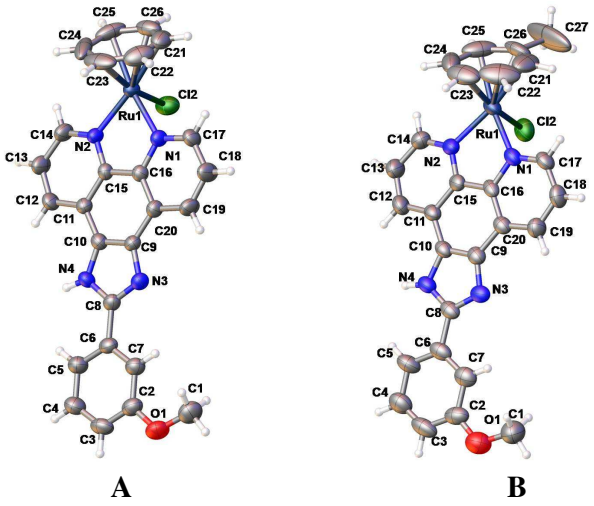

Fig.1 The molecular structure of the lattice and the atom numbers of **1** and **2**

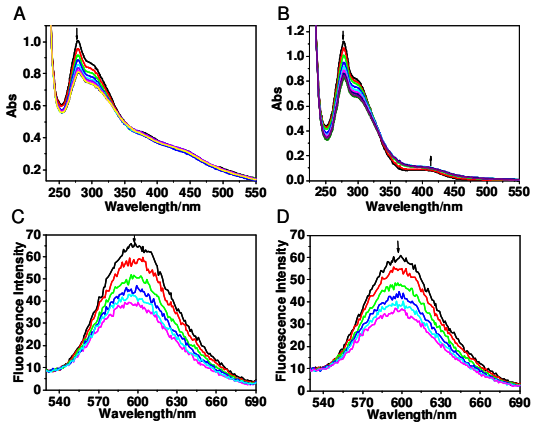

Fig.2 The study of interaction between arene Ru(II) **1** and **2** with *c-myc* G4 DNA by Spectroscopic methods. The electronic spectra of arene Ru(II) complex **1** (A) and **2** (B) in the absence and presence of *c-myc* G4 DNA, [Ru] = 20 μM. Emission spectra of EB and *c-myc* G4 DNA in the incubation buffer in the absence and presence of **1** (C) and **2** (D), [EB] = 16 μM, [DNA] = 2 μM.

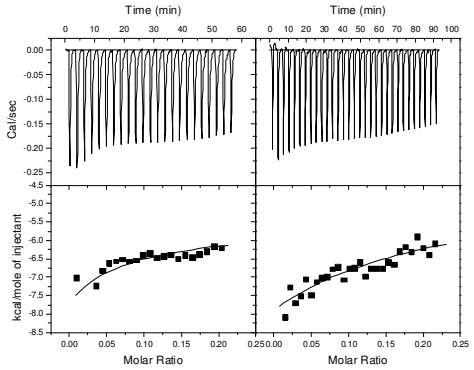

Fig. 3 ITC experimental curves at 25 °C for titration of **1** (left) and **2** (right) with *c-myc* G4 DNA. Results were converted to molar heat and plotted against the compound/DNA molar ratio. The line shows the fit to the results and gives the best-fit ΔH values for binding, [DNA] = 2 μM.

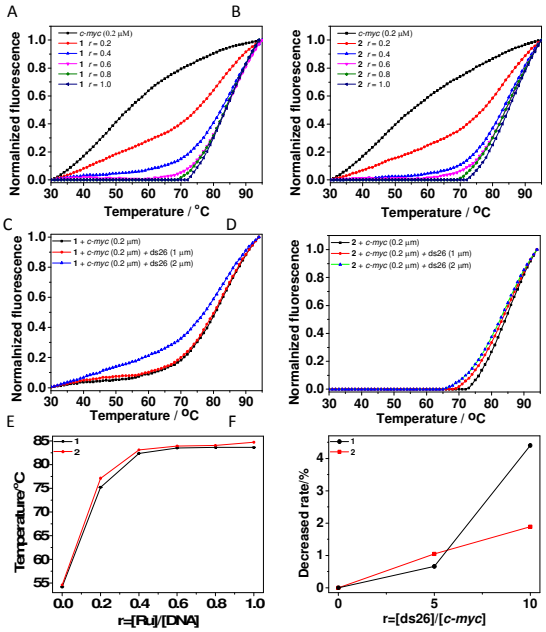

Fig. 4 FRET-melting curves obtained with *c-myc* G-quadruplex DNA (0.2 μM) alone (■) upon addition of **1** (A) and **2** (B). Competive FRET-melting curves obtained with *c-myc* G-quadruplex DNA (0.2 μM) and **1** (0.2 μM) (■) upon addition of ds26 DNA (C), for **2** (D). The increasing trend of *c-myc* melting upon the addition of **1** and **2** (E), r=[Ru]/[*c-myc*]=0, 0.2, 0.4, 0.6, 0.8 and 1.The selective binding affinity of **1** and **2** between *c-myc* G-quadruplex DNA and ds26 duplex DNA (F). Y-axis: the decreased rate of *c-myc* melting; X-axis: the concentration ratio of [ds26]/[*c-myc*]

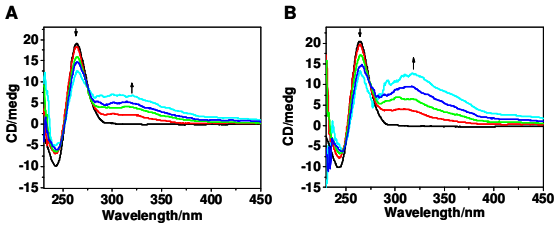

Fig. 5 CD titration spectra of *c-myc* G4 DNA (2 μM) at different concentrations of **1** (A) and **2** (B) in the incubation buffer.

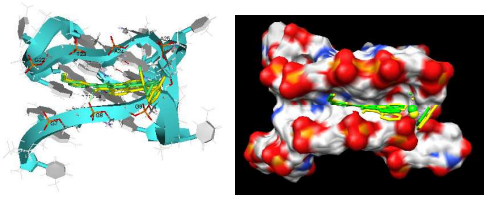

A B

Fig. 6 The binding site (A) and binding mode (B) of complex 1 and 2 with *c-myc* G4 DNA caculated by molecular docking

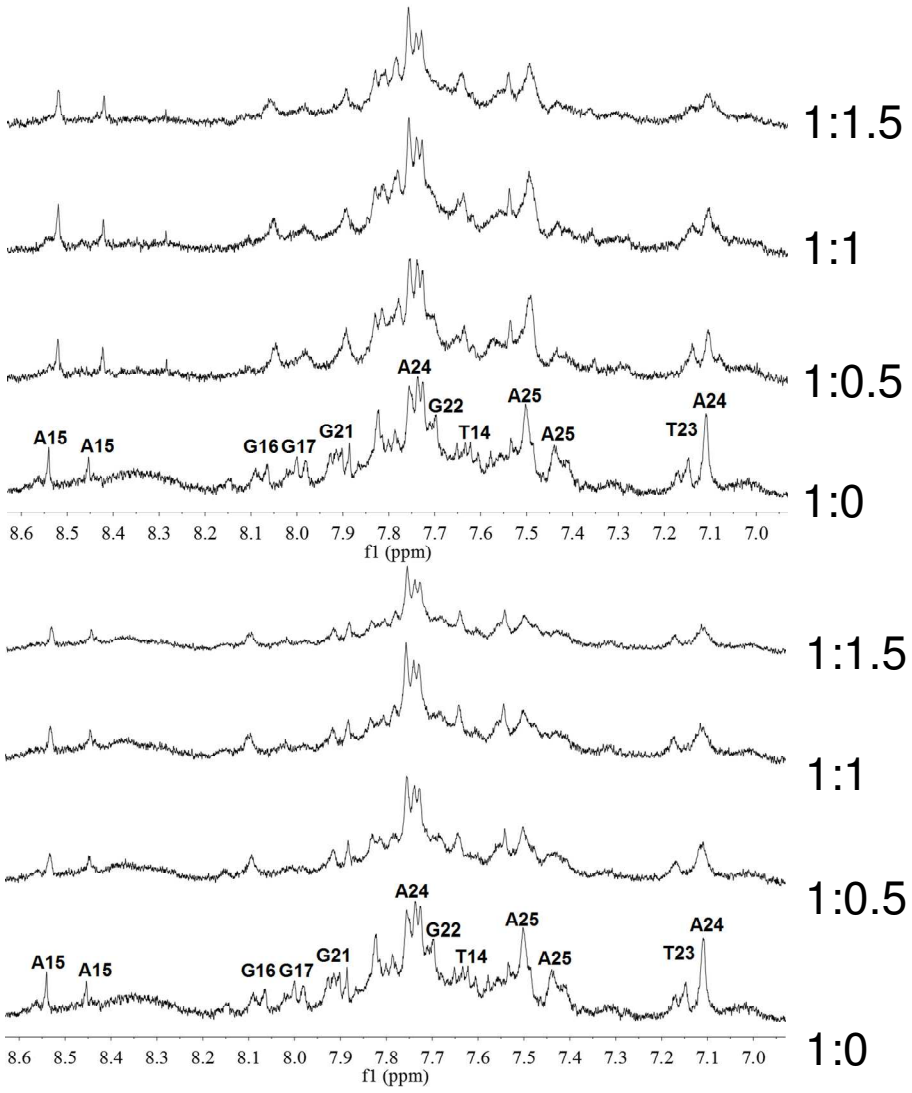

Fig. 7 The ^{1}H NMR spectra of *c-myc* treated with different concentration of **1** (A) and **2** (B). [*c-myc*]=100 μM, [Ru]=0, 50, 100 and 150μM.

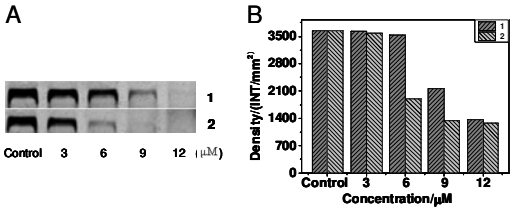

Fig. 8 (A) Effect of complex **1** and **2** on the PCR-stop assay with *c-myc* G4 DNA. [Ru]=0, 3, 6, 9, and 12 μM, [*c-myc*]=10 pM. (B) The replication blocking of PCR products obtained for different complex concentrations.

Table 1. Inhibitory effect of arene Ru(II) complexes on human liver cancer and normal cells.

Complex	IC_{50} (μM)		Toxicity index*
	HepG2	LO2	
1	48.8	212.4	4.4
2	43.7	129.1	2.9
m-MOPIP	42.2	34.9	0.83

* Toxicity index = IC_{50} (LO2)/ IC_{50} (HepG2).

Table 2. Binding constants and experimental thermodynamic values at 25 °C for interactions of **1** and **2** with *c-myc* G4 DNA

Comp.	$K_1(M^{-1})$	$K_2(M^{-1})$	ΔH_1 (cal/mol)	ΔH_2 (cal/mol)	$T\Delta S_1$ (cal/mol)	$T\Delta S_2$ (cal/mol)	ΔG_1 (cal/mol)	ΔG_2 (cal/mol)
1	1.21×10^3	/	-5.5	/	1.6	/	-7.1	/
2	1.10×10^3	3.62×10^5	-5.7	-9.6.	1.3	3.2	-7.0	-12.8